Quantifying The 3D Ground Deformation Induced By The 2010 El-Mayor Cucapah Earthquake Using Multi-Angle High Resolution Optical Imagery

S. Leprince (Caltech), F. Ayoub (Caltech), J. Hollingsworth (USC), J.P. Avouac (Caltech), and J. Dolan (USC)

Abstract:

We demonstrate how 3D ground deformations can be recovered using multi-angle, high resolution, satellite imagery, such as provided by the Quickbird or Worldview satellites. In particular, we apply this technique to reconstruct the 3D displacement field induced by the Mw 7.2 2010 El-Mayor Cucapah earthquake. Full-field ground deformation is recovered using sub-pixel image matching and triangulation on a set of images acquired before the earthquake, and on a set of images acquired after the earthquake. This technique is implicitely equivalent to reconstructing two elevation models, before and after the earthquake, using stereoscopy, and matching them. We show that the results compete with the analysis of the pre and post-earthquake LiDAR acquisitions.

Multi-Angle Stereo Processing

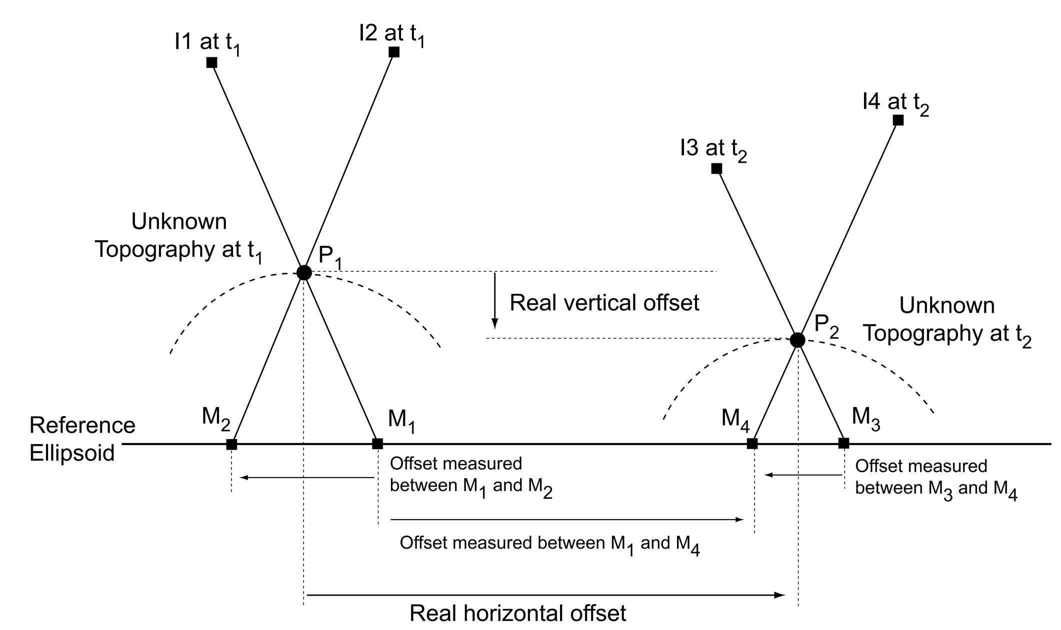

Pre-earthquake Images:

- Quickbird 09/21/2006
  Along-track angle: -1.23°
  Across-track angle: -9.8°
- Worldview 09/16/2008
  Along-track angle: -10.8°
  Across-track angle: 13.5°
- Worldview 01/10/2008
  Along-track angle: 13.8°
  Across-track angle: -2.1°

Post-earthquake Images:

- Worldview 04/10/2011
  Along-track angle: -13.8°
  Across-track angle: -22.5°
- Worldview 05/19/2011
  Along-track angle: 14.1°
  Across-track angle: 21.6°
- Worldview 10/10/2011
  Along-track angle: -25.8°
  Across-track angle: -1.9°

Given two pairs of stereo images (I1, I2) and (I3, I4), respectively acquired at times t1 and t2, the 3D displacement of the topographic surface can be retrieved from the apparent offsets between each image pair measured via sub-pixel correlation [Leprince et al, 2007]. If the topography of the surface is unknown, the point P1 will be seen in images I1 and I2, but respectively projected at M1 and M2 on a reference ellipsoid. After a deformation occurs, P1 will be displaced to P2, which will be projected at M3 and M4 from I3 and I4. Knowing the position of the optical center of the imaging systems, the 3D position of P1 and P2 can be triangulated, from which the 3D displacement vector from P1 to P2 is deduced.

LiDAR Processing

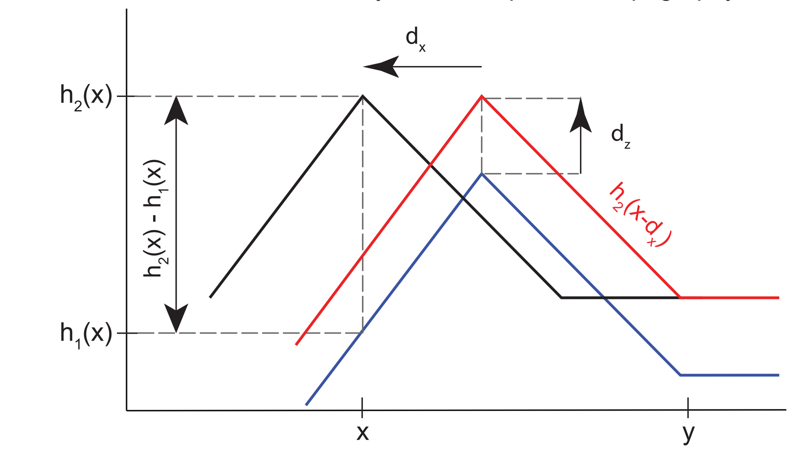

(1) $h_2(x) - h_1(x) = h_1'(x)d_x + d_z$ (2) $h_2(x - d_x) - h_1(x) - d_z$

Pre-earthquake LiDAR (average point cloud density .013 points/m^2) acquired in 2006 by INEGI was interpolated into a grid at 5m resolution by CICESE. Post-earthquake high resolution (9 to 18 returns/m^2) LiDAR was collected by NCALM [Oskin et al., 2010] in mid-August, 2010 and was delivered via the OpenTopography website.

The post-earthquake point cloud was arranged into buffered tiles using the open library libLas (liblas.org), in combination with the free LASTool software . The ENVI plug-in "BCAL LIDAR Tools" was then used to grid, without edge effects, the post-earthquake point clouds on a 5m post-spacing grid aligned with the pre-earthquake 5m Lidar grid.

To estimate the relative horizontal offsets between the pre- and the post-earthquake LiDAR DEMs, we used the sub-pixel phase correlation algorithm provided in COSI-Corr [Leprince et al, 2007]. The post-earthquake DEM is then warped onto the pre-earthquake DEM according to the relative horizontal offset field measured, producing $h_2(x - dx)$. The vertical offset is retrieved without bias by differencing the post-earthquake LiDAR DEM, compensated for horizontal motion, with the pre-earthquake LiDAR DEM.

Multi-Angle Stereo Processing Results

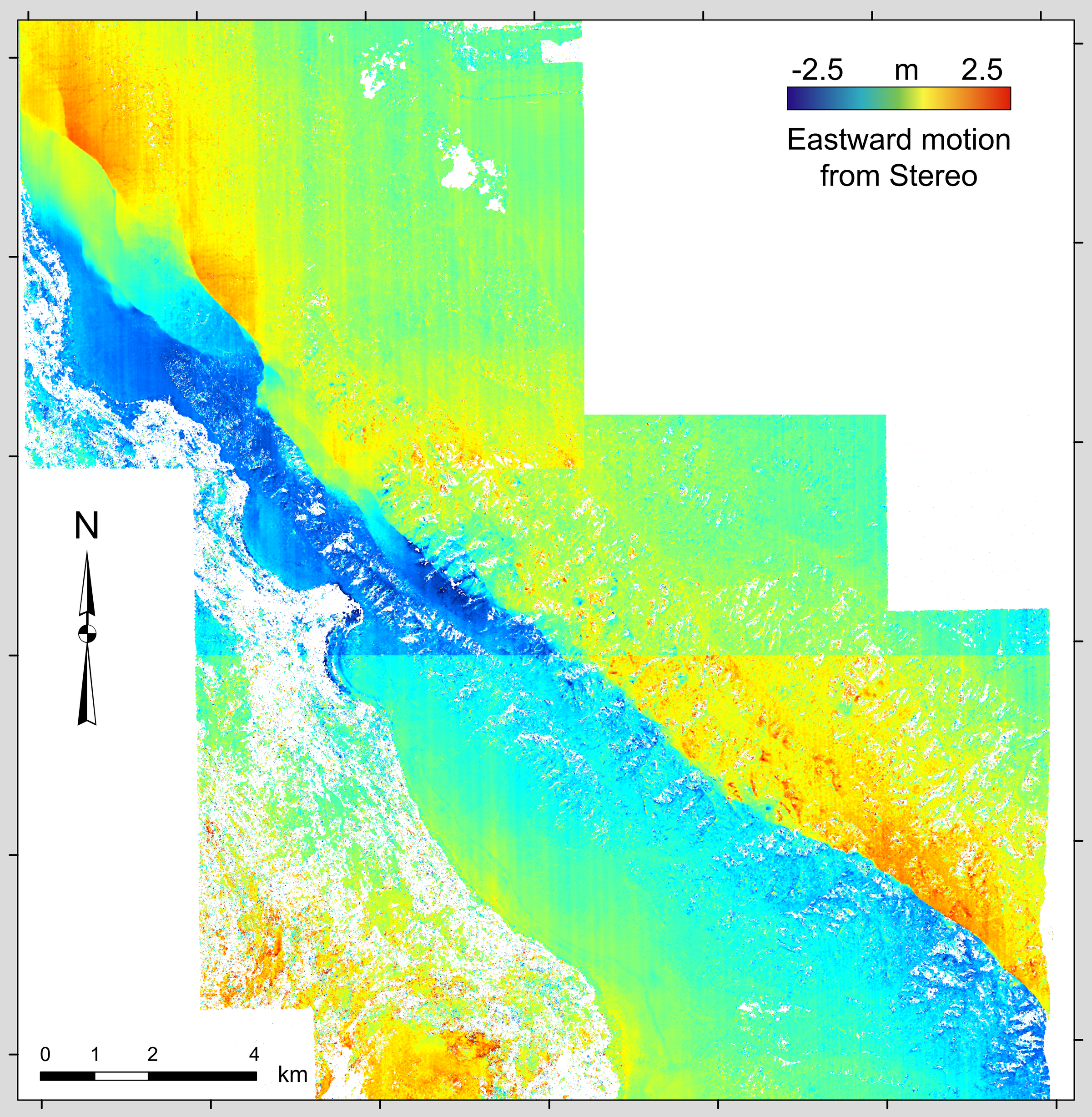

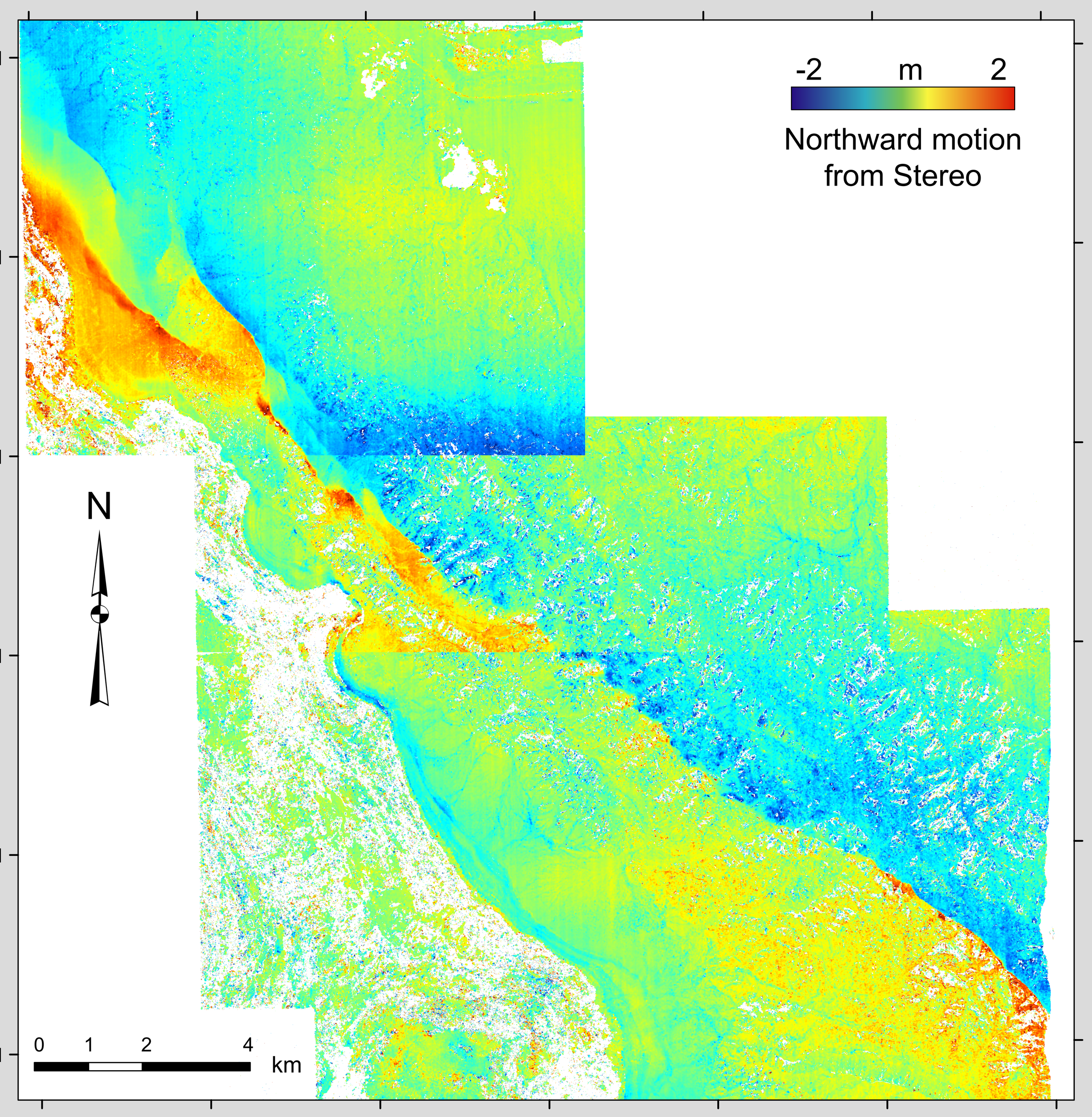

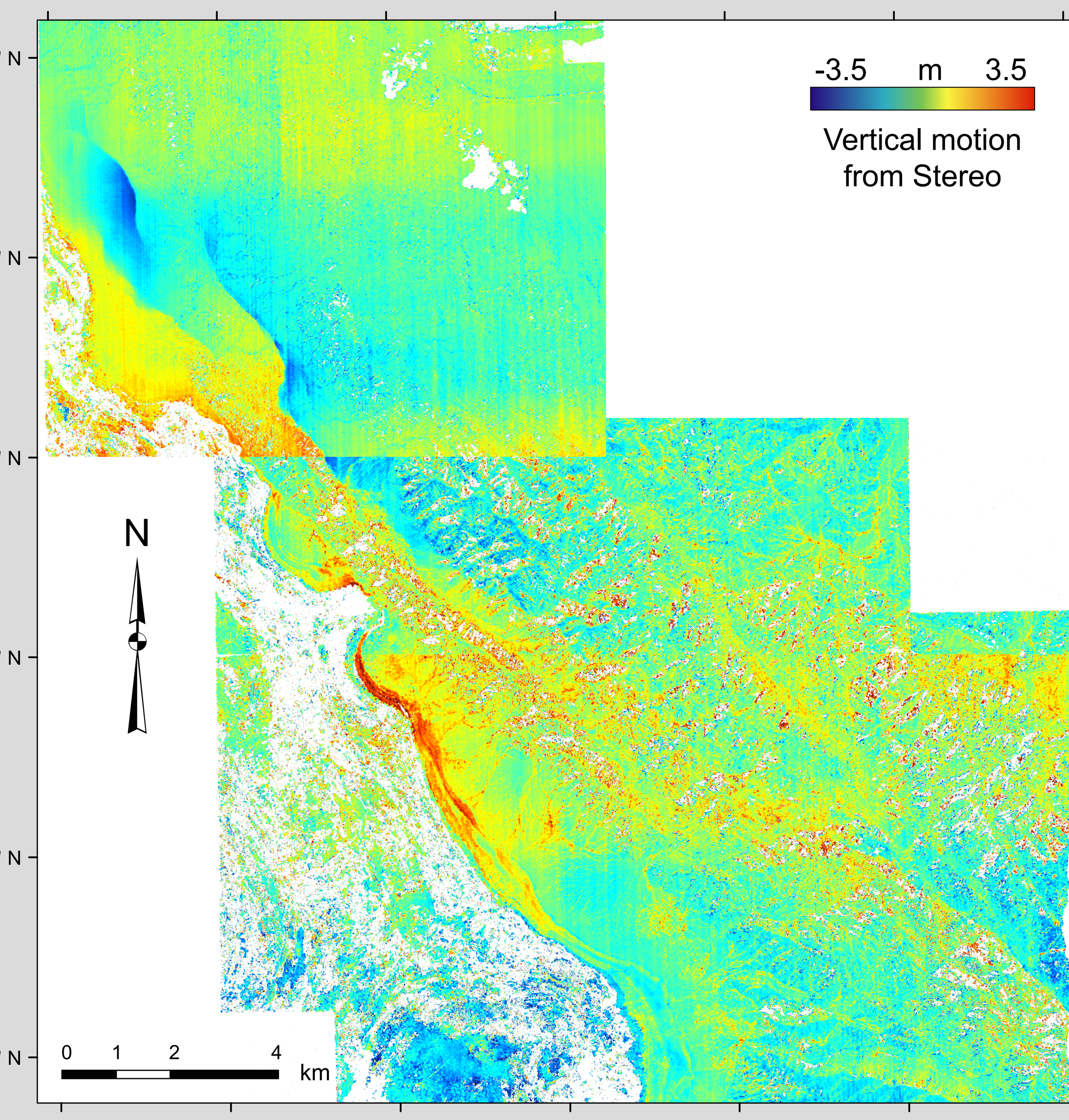

32°32' N
32°30' N
32°28' N
32°26' N
32°24' N
32°22' N

115°40' W 115°38' W 115°36' W 115°34' W 115°32' W 115°30' W 115°28' W

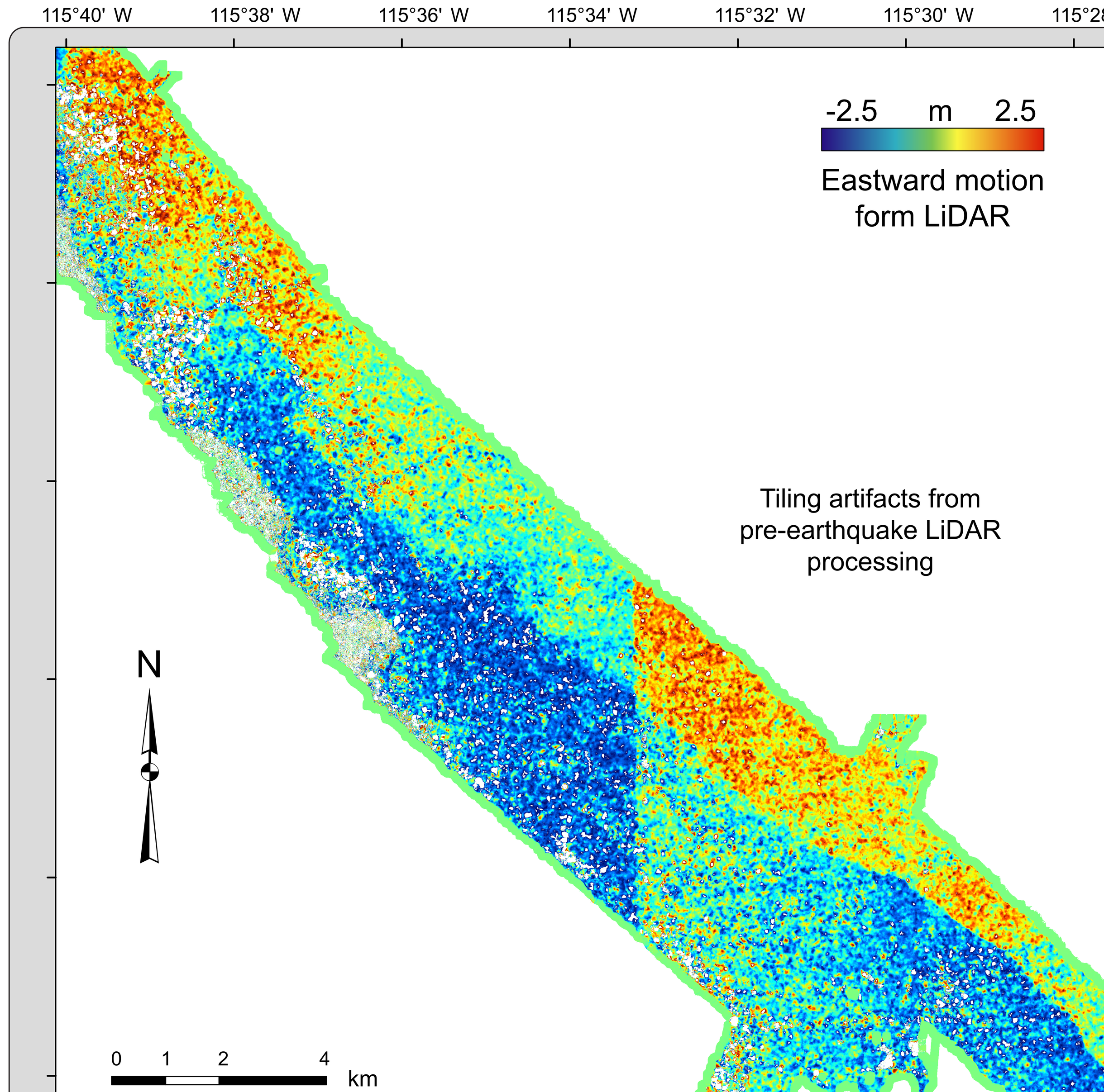

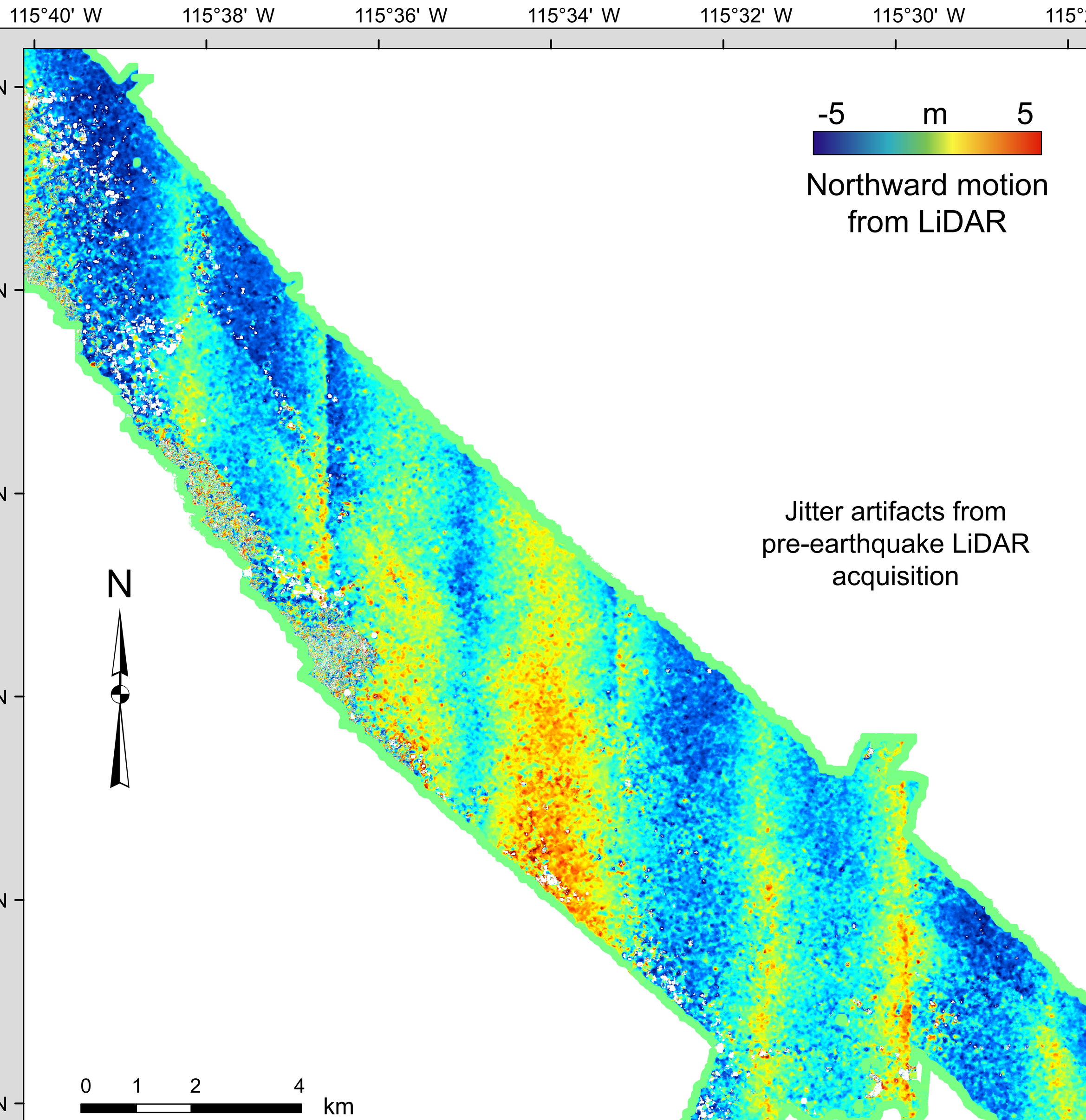

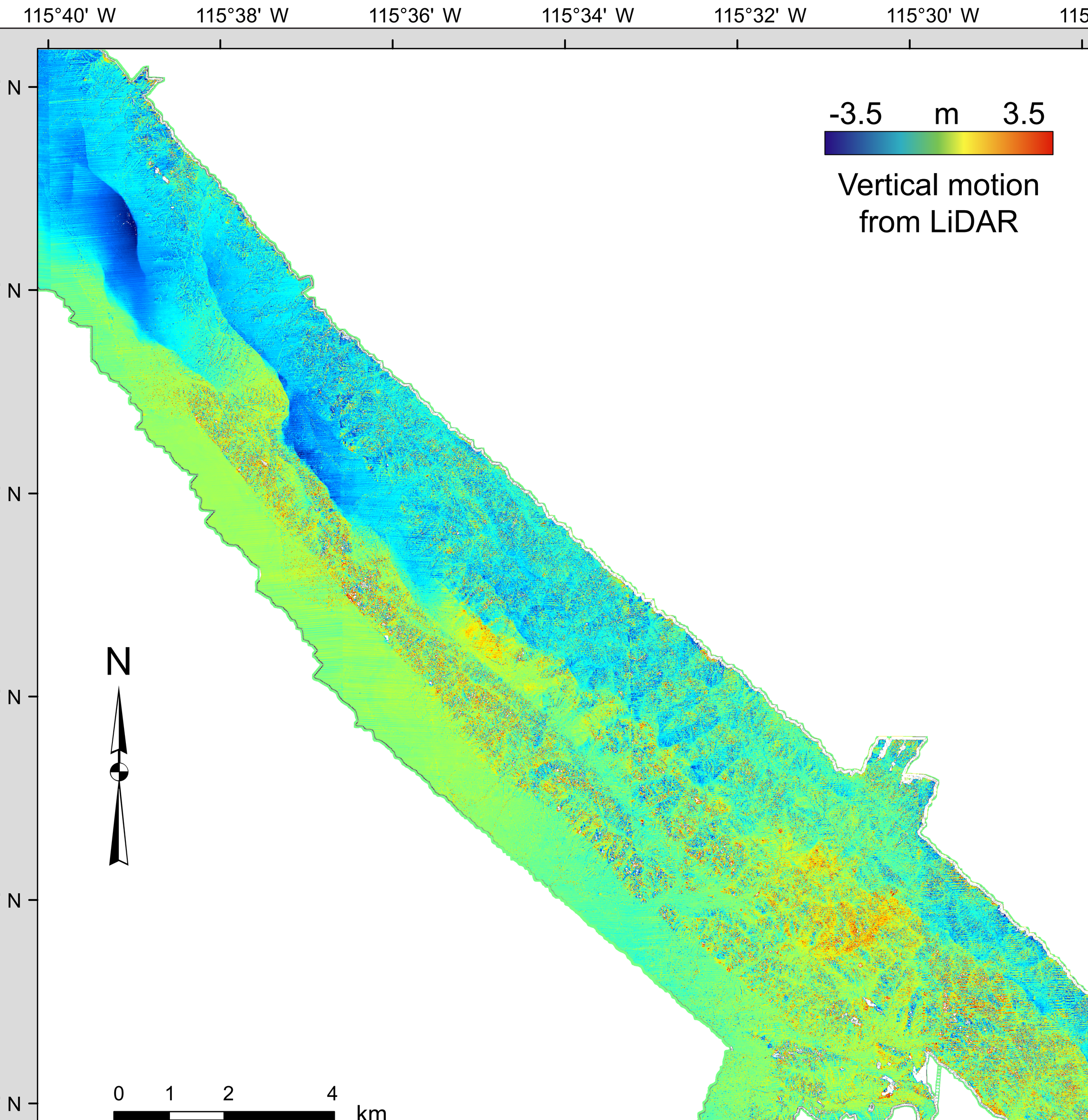

LiDAR Processing Results

Results in from work with K. W. Hudnut (U.S.G.S.), S. Akciz (UCI), A. Hinojosa Corona (CICESE), and J. M. Fletcher (CICESE)

Conclusions:

- The processing of multi-angle, high-resolution, satellite imagery, appears as a robust alternative to LiDAR acquisitions to quantify ground deformation induced by large earthquakes.
- The 0.5 m stereo imagery processing delivers results of overall higher fidelity than can be obtained using a 5 m LiDAR data set. Indeed, the worst result from the stereo imagery is given in the vertical component of the deformation field, which compares in quality to the best result provided by the LiDAR analysis.
- No particular imagery tasking was necessary to carry the stereo processing as all images were readily available in the Worldview and Quickbird archives. Better results could have been obtained if along-track, simulataneous, stereo acquisitions had been tasked.
- The multi-stereo processing was done at low cost thanks to the free access to the Worldview and Quickbird archive via the National Science Foundation.

References:

S. Leprince, S. Barbot, F. Ayoub and J. P. Avouac, "Automatic and Precise Ortho-rectification, Coregistration, and Subpixel Correlation of Satellite Images, Application to Ground Deformation Measurements," IEEE Transactions on Geoscience and Remote Sensing, Vol.45, No.6, June 2007.

S. Leprince, K. W. Hudnut, S. Akciz, A. Hinojosa Corona, and J. M. Fletcher, "Surface rupture and slip variation induced by the 2010 El Mayor – Cucapah earthquake, Baja California, quantified using COSI-Corr analysis on pre- and post-earthquake LiDAR acquisitions," AGU Meeting, Dec. 2011.

M. E. Oskin, J R. Arrowsmith, A. Hinojosa Corona, A. J. Elliott, J. M. Fletcher, E. Fielding, P. O. Gold, J. J. Gonzalez Garcia, K. W. Hudnut, J. Liu-Zeng, O. J. Teran, "Near-Field Deformation from the El Mayor–Cucapah Earthquake Revealed by Differential LIDAR," Science, Vol. 335 no. 6069 pp. 702-705, 10 Feb., 2012.